

Morphological and molecular effects of trace metals on parenchymatous organs of diabetic rat model

Ahmed S. Ahmed

Anatomy and Embryology Department, College of Medicine, Tanta University, Tanta 31511, Egypt

SUMMARY

Trace metals are naturally materials found in water, earth crust and rocks, making the exposure rate to these metals is high affecting vital organs of the body. Diabetes is an endocrinal disease that can also affect many body organs by its oxidative stress like action. The present study was conducted to examine the effect of various trace metals on some parenchymatous organs in a diabetic and non-diabetic rat model. 120 Albino Wistar rats were used, and diabetes was induced in 60 rats. All rats were divided into twelve groups. All of them received trace metals for 4 weeks, except the control groups. At the end of the study, samples from blood (for biochemical analysis), heart, pancreas, liver, kidney and spleen (for histopathological and gene expression analysis) were collected. All trace-metal-treated groups showed histopathological insult and functional disability. The extent of injury was extensive in diabetic groups if compared to non-diabetic groups. The genetic expression analysis showed increase in apoptotic genes CASP-3 and a marked decrease of anti-apoptotic genes BCL-2. The present study showed that trace metals are highly toxic to various organs of the body even in low concentration. The diabetic rats are more susceptible to trace-metal-induced cellular damage through gene-mediated pathway. CASP-3 gene plays an important role in trace-metal-associated tissue injury. The present study showed

that cadmium affects mainly hepatic and splenic tissues. Chromium, arsenic and thallium affect mainly the kidney, heart and pancreas respectively.

Key words: Trace metals – Parenchymatous organs – Apoptosis – CASP-3 – BCL-2

INTRODUCTION

Diabetes mellitus (DM) is an endocrinal disorder characterized by a sustained elevation of blood glucose level, if uncontrolled, it can cause cardiovascular, renal and hepatic complications due to its effect on microvasculature. As estimated in 2017, 450 million people are affected with diabetes. World health organization (WHO) reported that diabetes causes about six million deaths per year (Piepoli et al., 2016). Economically speaking, diabetes-related expenditures in 2019 exceeded one billion dollars. The average cost of diabetic patients is three-fold nondiabetic personnel (Ashrafzadeh and Hamdy, 2019). Its classic symptoms include polyuria, polyphagia and polydipsia, together with symptoms of multi-organ complications. Diabetes affect the cardiovascular system and it doubles the risk of cardiovascular complications (Bettencourt-Silva et al., 2019). It affects small blood vessels of the eye, brain, kidney and the peripheral nervous system, causing blindness, stroke, nephropathy and peripheral neuropathy respectively (Westerberg, 2013). The main cause of diabetes is insulin

Corresponding author:

Ahmed S. Ahmed, 13 Al-Bahr street, Tanta (31511), Gharbia, Egypt.
E-mail: Ahmedsahmed.tanta@gmail.com

Submitted: May 7, 2020. Accepted: October 1, 2020

deficiency or insulin resistance, which result in glucose accumulation in the blood stream causing glycosuria, followed by polyuria (Gilardi et al., 2019).

Trace metal is an expression used to describe any metallic compound that is toxic in low concentrations and has high atomic weight, e.g., mercury, thallium, cadmium, chromium and arsenic (all have density more than 5 gm/cm³). These are found in water in very limited concentrations; if their concentration crosses specific limits, they can cause cardiac and renal complications (Hwang et al., 2018).

Mercury (Hg) is one of the trace metals discovered by ancient Egyptians in 1500 BC. Historically, mercury chloride was used as a diuretic and disinfectant, as well as in syphilis treatment. It is still used in thermometers, barometers, sphygmomanometers, fluorescent light lamps and in the cosmetics industry (Kern et al., 2016) In some developing countries it is also still used in dentistry in the form of metal mixture amalgam (Andreoli and Sprovieri, 2017). Other modes of exposure include Hg toxicity during wars, as Hg is used in explosives production, or by eating fish like shellfish or tuna, which can store considerable amount of mercury (Bose-O'Reilly et al., 2017). Some water-soluble forms of Hg are present such as methylmercury, which can cause toxicity if ingested (Siblerud et al., 2019). It can be absorbed through the skin, the gastrointestinal mucous membrane and olfactory mucous membrane if mercury vapors are inhaled or during tobacco smoking (El-Badry et al., 2018). It is extremely toxic and can damage the central nervous system, kidneys, liver, lungs and other organs. The toxic effect is dose related (Vianna et al., 2019).

Thallium (Ti) is a trace metal discovered in 1861. It is used in pharmaceutical, cosmetics and glass industries, and also as a (tasteless) poison. Medically, it is used in cardiographs to examine the coronaries and the state of heart revascularization after graft surgeries. It is absorbed readily by the skin and the mucous membrane of either the gastrointestinal or respiratory tracts (Campanella et al., 2019). Cadmium (Cd) is a silvery, white and solid trace element. Discovered in 1817 in Germany. It is commonly used in batteries, pigments, the electric industry, television screen manufacturing, anticancer drugs, laser emission

and immunofluorescent microscopes. It can cause cellular oxidative stress. Intoxication of cadmium can be caused by inhalation of fertilizers causing pulmonary edema (Wu et al., 2019).

Chromium (Cr) is the most abundant trace metal in the earth crust and rocks, discovered in 1797. It is used in pigment manufacturing and as a metal surface coating. In laboratories, it is used to clean glass containers (Them et al., 2018). Arsenic (As) is one of the oldest trace metals: discovered in 815 AD, it was described by the Arab chemist Jabir Ibn Haiyan. It is used in wood preservation, insecticides and in rat poisons. It is highly soluble and easily absorbed. Historically it was used in syphilis treatment and as an antibiotic (Karbowska, 2016).

All previously mentioned trace metals cause cellular stress through oxidative stress and ignition of cellular apoptosis. The programmed cell death [apoptosis] is regulated by genetic factors such as CASP-3 [apoptotic gene] and BCL-2 [anti-apoptotic gene] (Beyaert et al., 1997). Thus, the present work is designed to examine the effect of trace metals (Hg, Ti, Cd, Cr, As) on apoptosis-regulating genes (CASP-3, BCL-2) in diabetic and non-diabetic albino rats. The current study will also examine the effect of trace metals' toxicity on both the function and histological structure of the liver, heart, kidney, pancreas and spleen.

MATERIALS AND METHODS

Chemicals

20 gm of mercury Bi-chloride, 95% (HgCl₂), 20 gm of thallium Bi-chloride, 95% (TiCl₂), 20 gm of cadmium Bi-chloride, 95% (CdCl₂), 20 gm of chromium Bi-chloride, 95% (CrCl₂) and 20 gm of arsenic Tri-chloride, 95% (AsCl₃) were purchased from Sino pharm Chemical Reagent Co., Ltd. (Shanghai Shi, China).

Animals

One hundred and twenty albino Wistar rats were used, with an average weight of 200 gm and an average age of 6 months. Animals were housed individually. Free access to food and water was allowed. A 12-hour light/dark cycle was kept. By the help of air conditions, the temperature was kept at

25°C (in accordance to national and institutional guidelines). This research study was approved by the Research and Ethics Committee, Quality Assurance Unit, Faculty of Medicine, Tanta University, Egypt.

Experimental design

Diabetes was induced by injecting streptozotocin 40mg/kg b.w., one-week later, blood glucose level was measured. Rat is considered diabetic if blood glucose level > 300 mg/dl. Rats were divided into twelve groups (n=10), Group I, control nondiabetic, Group II, Hg-nondiabetic, Group III, Ti-nondiabetic, Group IV, Cd-nondiabetic, Group V, Cr-nondiabetic, Group VI, As-nondiabetic, Group VII, diabetic, Group VIII, Hg-diabetic, Group IX, Ti-diabetic, Group X, Cd-diabetic, Group XI, Cr-diabetic, Group XII, As-diabetic.

All groups (except Group I and Group VII) received intraperitoneal injection of the respective trace metal salt 20 mg/kg b.w. twice weekly for four weeks. Group I and VII received intraperitoneal saline injection instead. At day 30, all rats were sacrificed, blood from heart chambers was collected, serum was separated by centrifugation (4000 rpm) and kept at -30°C for biochemical studies. Heart, kidney, liver, pancreas and spleen samples were collected and further divided into two groups. The first group of organs was fixed in 10% neural buffered formaldehyde, dehydrated, embedded in paraffine, then sectioned at 5 µm and stained with hematoxylin and eosin. The second group was homogenized and centrifuged for gene expression analysis using reverse transcriptase PCR (Pawłowska et al., 2017).

Histopathological examinations

Fresh tissue samples were cut into cubes (1 cm³), placed in fixative 10% paraformaldehyde solution, immersed in paraffine blocks, sectioned into 5 µm thick sections using CUT 4050 Microtome (Laborgeräte Microtec, Germany), and finally stained with hematoxylin and eosin. Histopathological examinations were performed by two histopathologists blinded to present study.

Biochemical analysis

Serum was analyzed for blood urea, creatine, Aspartate Aminotransferase of liver (ASTL), Alanine

Transaminase of liver (ALTL), random blood glucose, bilirubin and total cholesterol (Kits were purchased from Sino pharm Chemical Reagent Co.,)

Gene analysis

Following sacrificing rats, the heart, kidney, liver, pancreas and spleen tissues were harvested for gene expression analysis. RNA from tissues was extracted using Trizol reagent (Invitrogen, USA) and quantified with an ND-1000 spectrophotometer (NanoDrop Technologies, USA). cDNA was synthesized from 1 µg RNA with the Revert Aid H-Minus first-strand cDNA synthesis kit (Invitrogen, USA) as the manufacturer's protocol. The qRT-PCR analysis of all heavy-metal-treated groups, as well as the non-diabetic untreated control group, was carried out for Caspase-3 (apoptotic gene) and Bcl2 (anti-apoptotic gene) using Maxima SYBR Green qPCR Master Mix (Fermentas, USA) according to the manufacturer's protocol and run on PikoReal 96 real-time PCR (Thermo Scientific, USA). The relative gene expression analysis was performed by using PikoReal software (Thermo Scientific). β-actin was used for normalization. Note: Caspase-3; forward primer: 5'-GGA CAG CAG TTA CAA AAT GGA TTA-3', reverse primer: 5'-GTCGATGCAGTCTCAGCTCTCA-3. Bcl2; forward primer: 5'-AAG CCG GCG ACG ACT TCT-3', reverse primer: 5'-GCCTACTCCTCAGTCTCTC-3'.

β-actin; forward primer: 5'-GCTGCCTGCTGACTAGT AT-3', reverse primer: 5'-CGTGTGTATGCTCTGACTAC-3'. PCR conditions were [initial denaturation at 96 °C (four min.), then forty cycles of 96 °C (twenty sec.), 63 °C (thirty sec.), and 72 °C (thirty sec.)]

Statistical analysis

Statistical Package for Social Sciences (SPSS) software, 20 V. (SPSS Inc., USA) was used for data analysis. The statistical significance of differences between groups was validated using one-way analysis of variance (ANOVA). Post hoc Scheffe's procedure was used for groups comparison. Data were expressed in mean ± standard deviation and probability value was considered significant if <0.05.

RESULTS

Heart

On examination of hematoxylin- and eosin-stained heart sections, the control group (G-I) showed normal histological architecture, normal cardiac myofibril with large prominent nuclei with clear intercalated discs with no capillary congestion. The diabetic group (G-VII) showed moderate tissue fibrosis, necrosis and cytoplasmic vacuolations. Trace-metal-treated nondiabetic groups (G-II, III, IV, V, VI) showed cytoplasmic vacuolation of cardiomyocytes, the nuclei appear small and pyknotic with necrotic cardiac myofibrils (Fig. 1). These histopathological changes become more extensive in trace-metal-treated diabetic groups (G-VIII-XII) congestion of small blood vessels and capillaries (Fig. 1). The extensive damage appears in As-diabetic group (G-XII) was also confirmed by statistically significant ($p < 0.05$) increased CASP-3 and decreased BCL-2 expression. The fluctuation of expression become more extensive in diabetic trace-metal-treated groups (G-VIII-XII) if compared to non-diabetic trace-metal-treated groups (G-II-VI) (Fig. 2).

Kidney

Hematoxylin- and eosin-stained kidney sections showed that the control group (G-I) revealed normal glomeruli. Tubular lining epithelium appears healthy with prominent nuclei with no cytoplasmic vacuolations. Tubular degeneration appears in the diabetic group (G-VII). Trace-metal-treated groups either diabetic (more extensive) or nondiabetic, showed cytoplasmic vacuolation, edema, small pyknotic nuclei and congested blood vessels (Fig. 3). The gene expression analysis of the kidney tissue showed that the chromium-treated (diabetic) group (G-XI) scored the highest value for CASP-3 expression and the lowest value for BCL-2 expression (Fig. 4). While the rest of trace-metal-treated groups showed relative fluctuation of apoptotic and anti-apoptotic genes in favor of the apoptotic gene (CASP-3) if compared to control group (G-I). After trace metal administration, the biochemical analysis revealed a statistically significant ($p < 0.05$) increase in blood urea and creatinine either in diabetic or non-diabetic (Fig. 5): the highest value was recorded also in chromium treated group (diabetic)(G-XI), which emphasizes the histopathological findings.

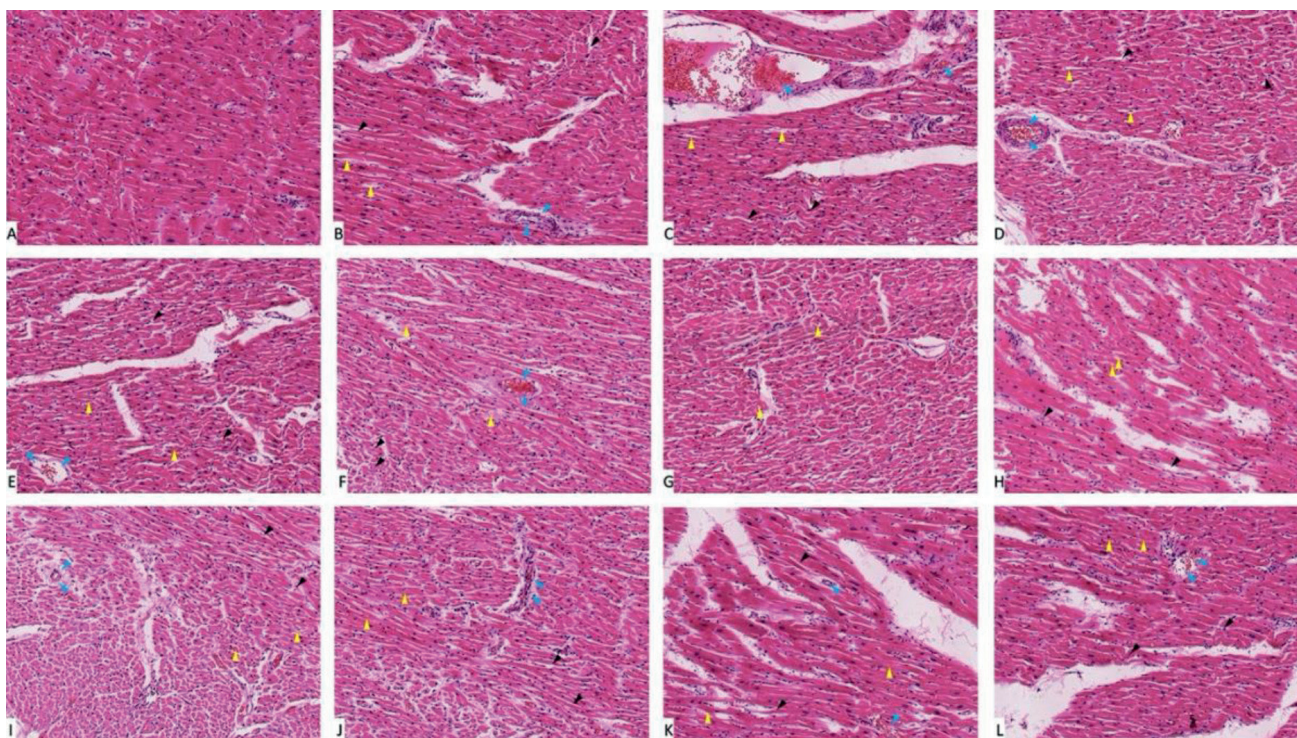


Fig. 1.- Heart tissue sections stained with hematoxylin and eosin (X 1000). (A) group I showed normal histological features. (B, C, D, E and F) represent nondiabetic groups treated with trace metals, group II, III, IV, V and VI, respectively. (G) represent diabetic non treated group VII. (H, I, J, K and L) represent diabetic groups treated with trace metals, group VIII, IX, X, XI and XII, respectively. Vacuolations are pointed at by yellow arrow, while degeneration and congestion are pointed into by black and blue arrows respectively.

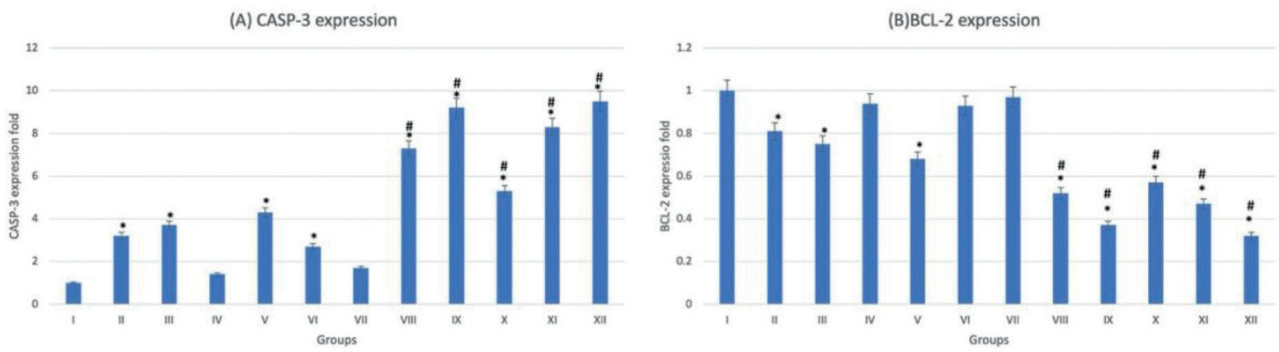


Fig. 2.- Gene expression analysis of the heart tissue of groups I-XII. **(A)** represent CASP-3. **(B)** represent BCL-2. * statistically significant ($p < 0.05$) difference in comparison to I-group. # statistically significant ($p < 0.05$) difference in comparison to VII-group. Data are presented as mean \pm standard deviation, (n=10).

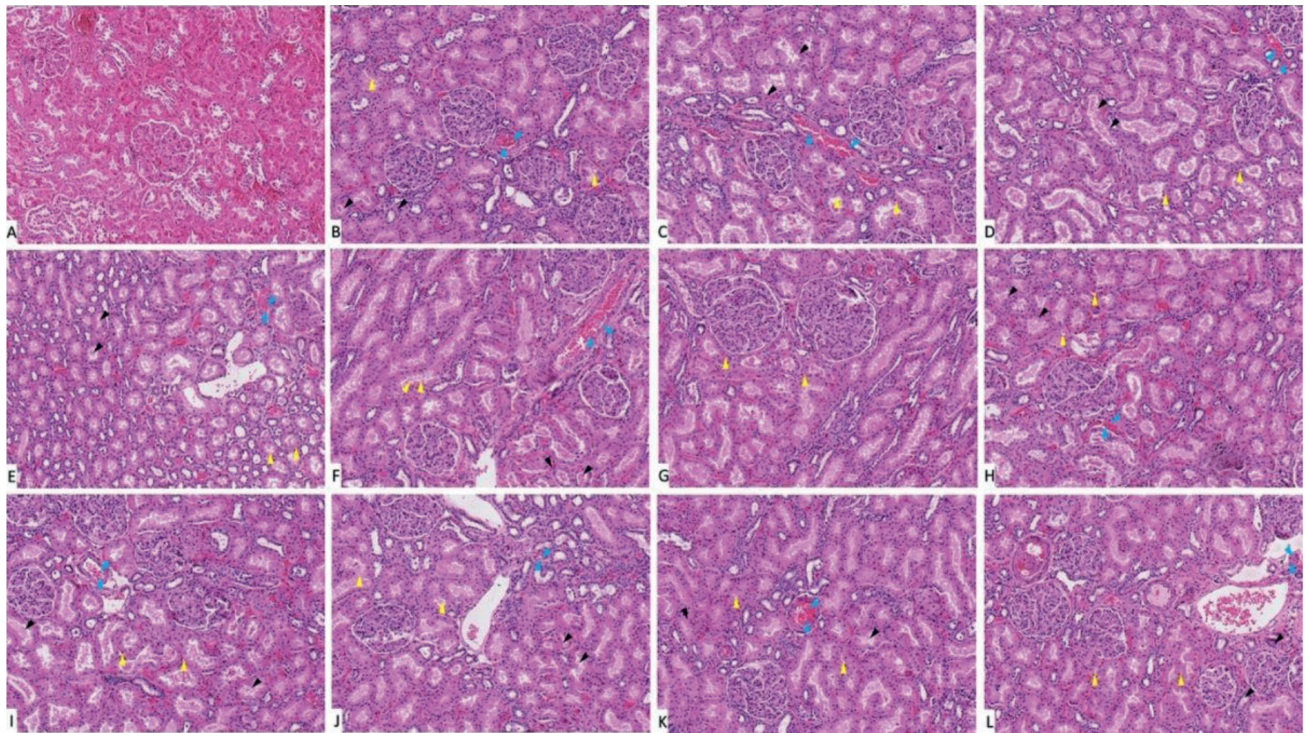


Fig. 3.- Kidney tissue sections stained with hematoxylin and eosin (X 1000). **(A)** Group I, showed normal histological features. **(B, C, D, E and F)** represent groups II, III, IV, V and VI, respectively. **(G)** represent diabetic non treated group VII. **(H, I, J, K and L)** represent groups VIII, IX, X, XI and XII, respectively. Vacuolations are pointed into by yellow arrow, while degeneration and congestion are pointed into by black and blue arrows respectively.

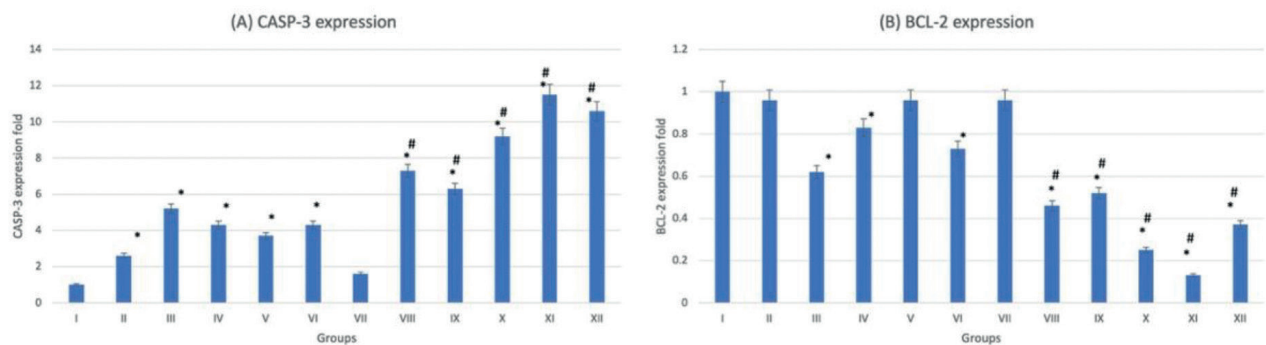


Fig. 4.- Gene expression analysis of the heart tissue of groups I-XII. **(A)** Represent CASP-3. **(B)** Represent BCL-2. * statistically significant ($p < 0.05$) difference in comparison to I-group. # statistically significant ($p < 0.05$) difference in comparison to VII-group. Data are presented as mean \pm standard deviation, (n=10).

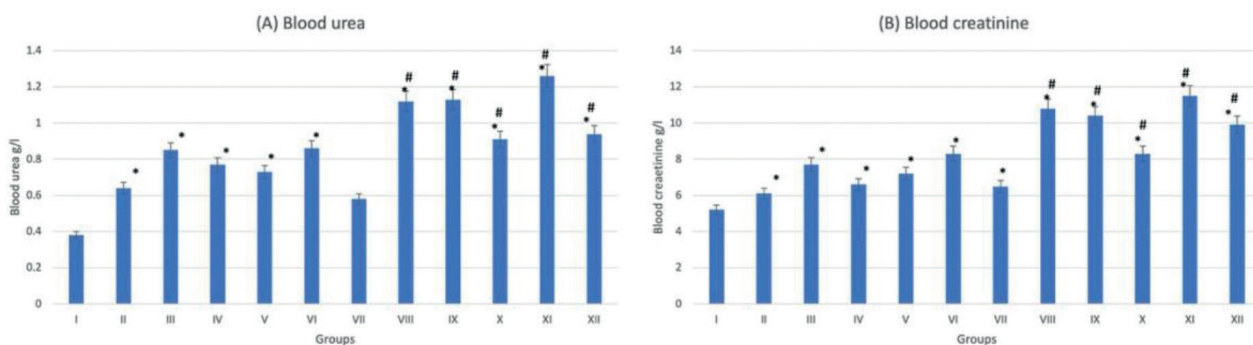


Fig. 5.- Kidney function tests of groups I-XII. (A) represent blood urea. (B) represent blood creatinine. * statistically significant ($p < 0.05$) difference in comparison to I-group. # statistically significant ($p < 0.05$) difference in comparison to VII-group. Data are presented as mean \pm standard deviation, (n=10).

Liver

On examination of hematoxylin- and eosin-stained liver sections, normal histological architecture was noticed in the control group (G-I) with characteristic hexagonal structure of liver lobule. Hepatocytes diverge from the central vein towards the periphery of the lobule. Hepatocytes appear healthy with normal cytoplasm and large central nuclei. Cellular degeneration and necrosis appeared in the diabetic non-treated group (G-VII). On administration of trace metals, especially in the cadmium group (G-XI), vacuolation and inflammatory cells infiltration appears in liver sections. These changes appeared more in

diabetic if compared to non-diabetic groups (Fig. 6). The gene expression analysis of CASP-3 and BCL-2 emphasizes the histopathological findings. In trace-metal-treated groups, [especially the cadmium group (G-X)] there was statistically significant ($p < 0.05$) increase in CASP-3 expression and decrease in BCL-2 expression (Fig. 7). Liver enzymes analysis (ASTL and ALTL) also emphasizes the histopathological findings denoting the functional affection of the liver after trace-metal administration in both diabetic and non-diabetic rats. The diabetic groups (trace metal treated) show more rise of enzymatic levels if compared to the non-diabetic (trace-metal-treated) groups (Fig. 8).

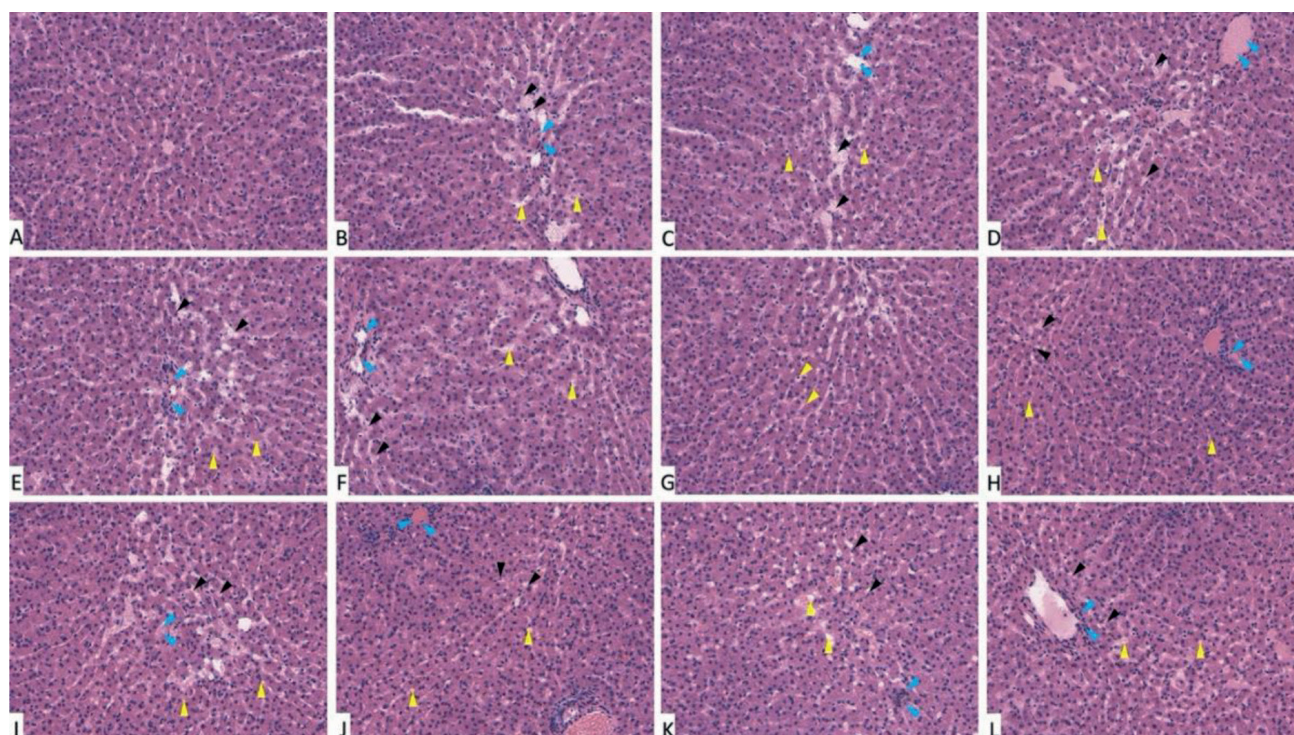


Fig. 6.- Liver tissue sections stained with hematoxylin and eosin (X 1000). (A) Group I showed normal histological features. (B, C, D, E and F) represent groups II, III, IV, V and VI, respectively. (G) represent diabetic non treated group VII. (H, I, J, K and L) represent groups VIII, IX, X, XI and XII, respectively. Vacuolations are pointed into by yellow arrow, while degeneration and congestion are pointed into by black and blue arrows respectively.

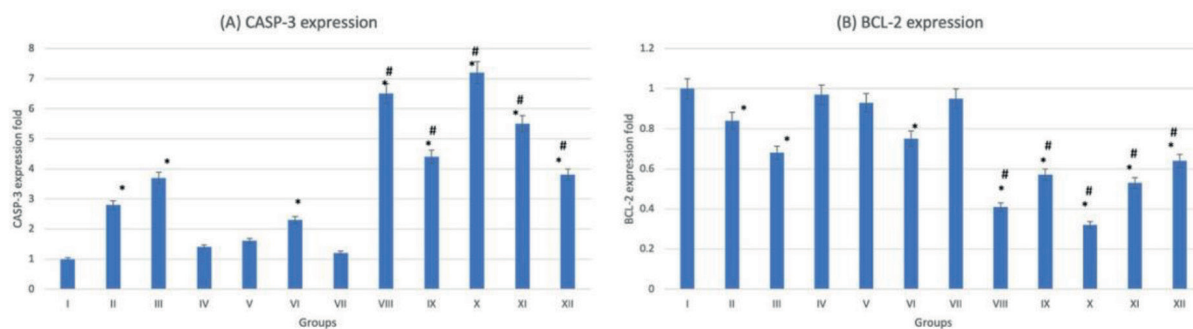


Fig. 7.- Gene expression analysis of the liver tissue of groups I-XII. (A) represent CASP-3. (B) represent BCL-2. * statistically significant ($p < 0.05$) difference in comparison to I-group. # statistically significant ($p < 0.05$) difference in comparison to VII-group. Data are presented as mean \pm standard deviation, (n=10).

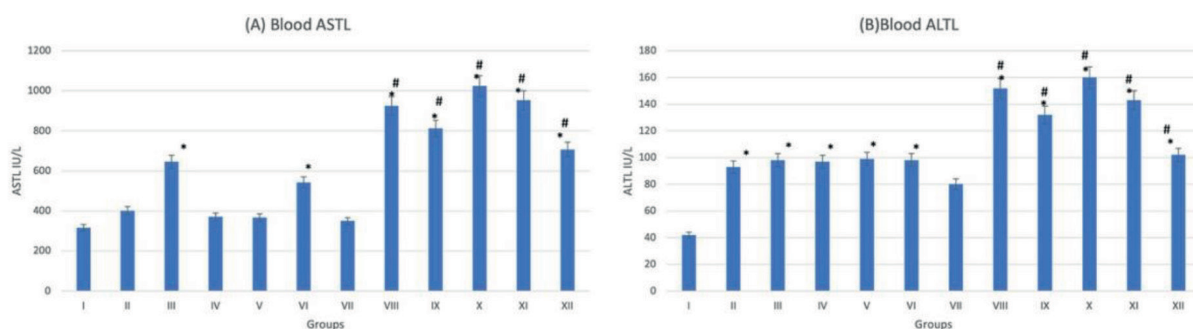


Fig. 8.- Liver function tests of groups I-XII. (A) Represent ASTL. (B) Represent ALTL. * statistically significant ($p < 0.05$) difference in comparison to I-group. # statistically significant ($p < 0.05$) difference in comparison to VII-group. Data are presented as mean \pm standard deviation, (n=10).

Pancreas

Examination of stained pancreas sections showed that the control group (G-I) has normal histological architecture with healthy acini and islet of Langerhans. In the diabetic group (G-VII), the acinar cells appear swollen with small cytoplasmic vacuolations. Cells appear shrunken, degenerative and necrotic in G-II-VI. Histopathological changes were more intense in diabetic groups treated with trace metals (G-VIII-XII). The thallium group (G-IX) showed extensive histopathological changes if compared to the rest of trace-metal-related groups, either diabetic or non-diabetic (Fig. 9). The gene expression analysis of pancreatic tissue confirmed the histopathological changes, more fluctuation of CASP-3 and BCL-2-fold levels either by increase and decrease respectively (Fig. 10). Biochemical study of the serum showed that group (G-IX) (thallium related) recorded the highest blood glucose score. All other groups (with exclusion of the control group) recorded elevated blood glucose levels (Fig. 11).

Spleen

The histological examination of splenic sections showed normal histological architecture in control group (G-I). All diabetic and non-diabetic groups showed congestion of red pulp after administration of trace metals together with cell necrosis of white pulp. The cadmium-treated diabetic group (G-X) showed the most extensive tissue injury if compared to the rest of groups (Fig. 12). This was confirmed by gene expression done to the splenic tissue, which showed that the cadmium-related group (G-X) scored the highest CASP-3 level among other groups (Fig. 13). As an indicator for splenic function, serum analysis for both bilirubin and total cholesterol levels were performed, which appeared to decrease after trace-metal administration either in diabetic or non-diabetic groups (Fig. 14).

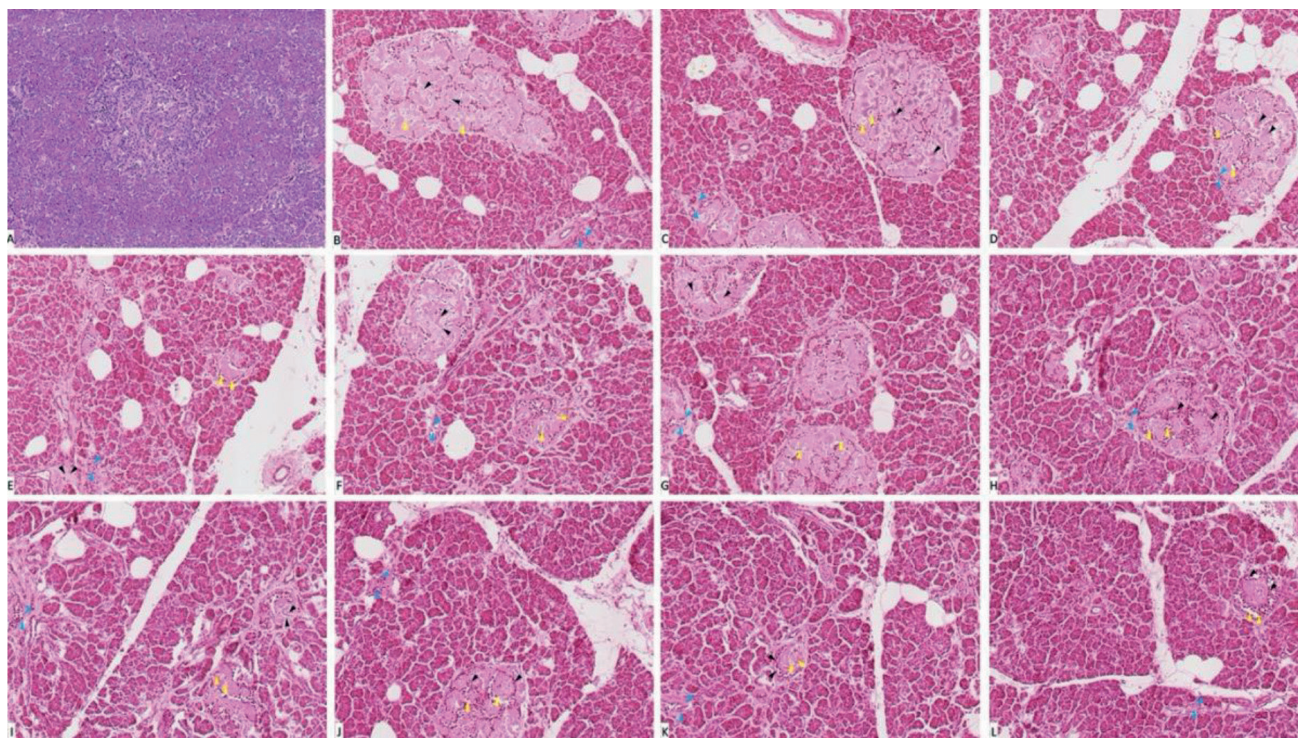


Fig. 9.- Pancreas tissue sections stained with hematoxylin and eosin (X 1000). (A) Group I showed normal histological features. (B, C, D, E and F) represent groups II, III, IV, V and VI, respectively. (G) represent diabetic non treated group VII. (H, I, J, K and L) represent groups VIII, IX, X, XI and XII, respectively. Vacuolations are pointed into by yellow arrow, while degeneration and congestion are pointed into by black and blue arrows respectively.

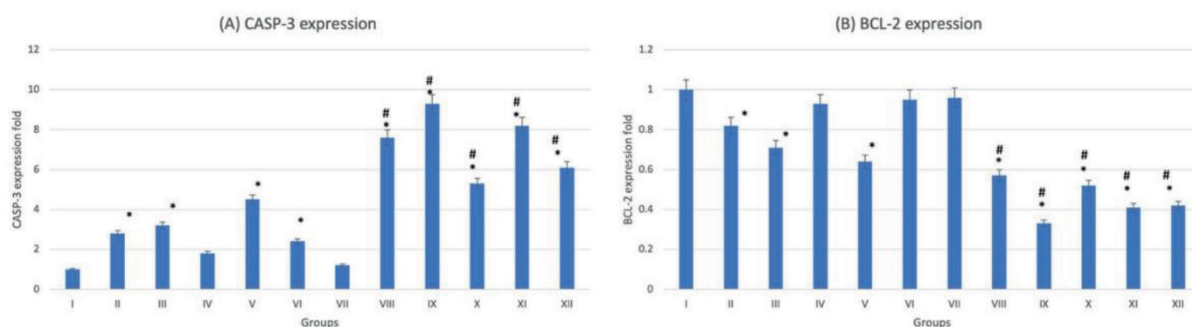


Fig. 10.- Gene expression analysis of the pancreatic tissue of groups I-XII. (A) represent CASP-3. (B) represent BCL-2. * statistically significant ($p < 0.05$) difference in comparison to I- group. # statistically significant ($p < 0.05$) difference in comparison to VII-group. Data are presented as mean \pm standard deviation, (n=10).

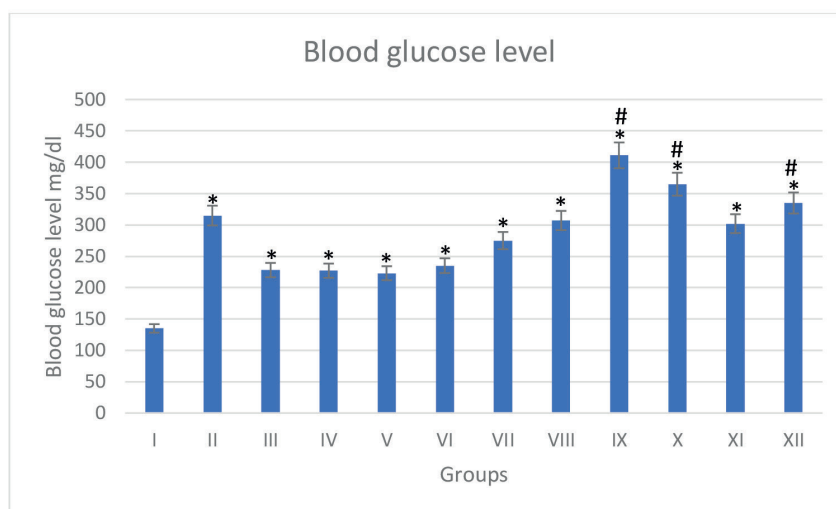


Fig. 11.- Blood glucose level of groups I-XII. * statistically significant ($p < 0.05$) difference in comparison to I-group. # statistically significant ($p < 0.05$) difference in comparison to VII- group. Data are presented as mean \pm standard deviation, (n=10).

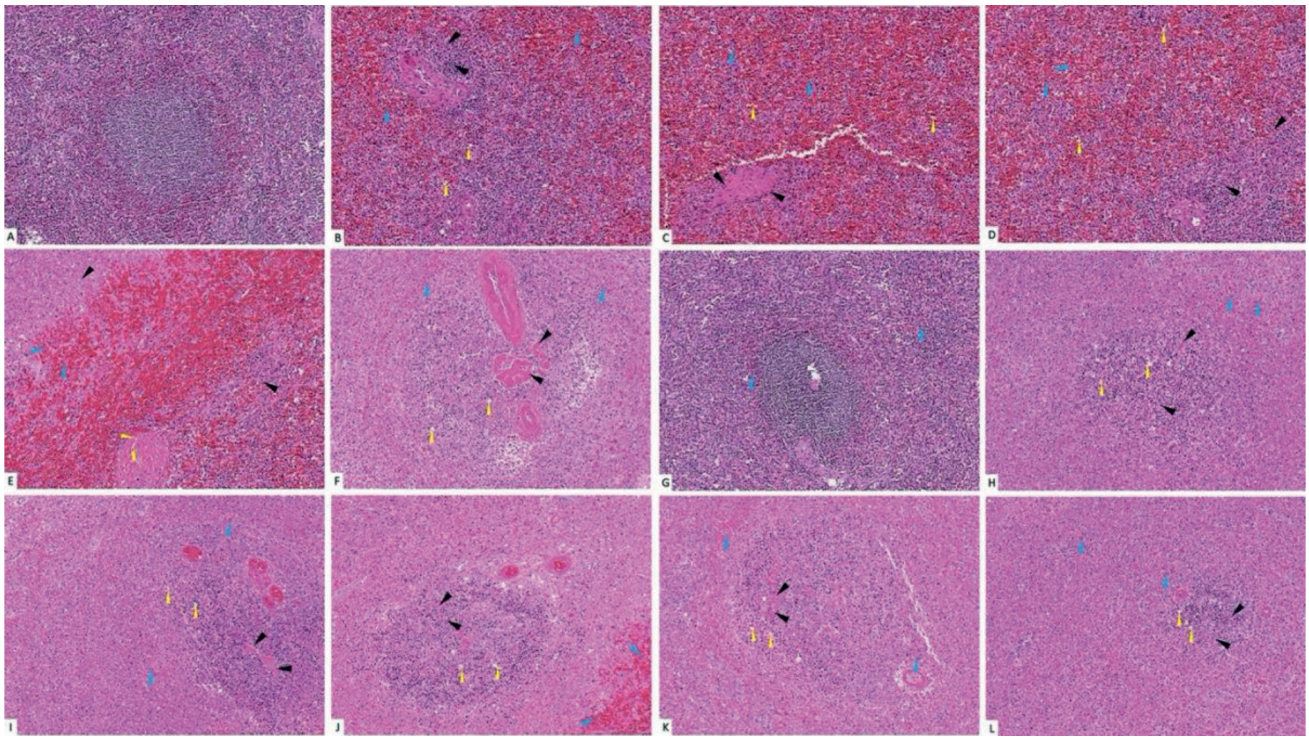


Fig. 12.- Splenic tissue sections stained with hematoxylin and eosin (X 1000). (A) Group I showed normal histological features. (B, C, D, E and F) represent groups II, III, IV, V and VI, respectively. (G) represent diabetic non treated group VII. (H, I, J, K and L) represent groups VIII, IX, X, XI and XII, respectively. Vacuolations are pointed into by yellow arrow, while degeneration and congestion are pointed into by black and blue arrows respectively.

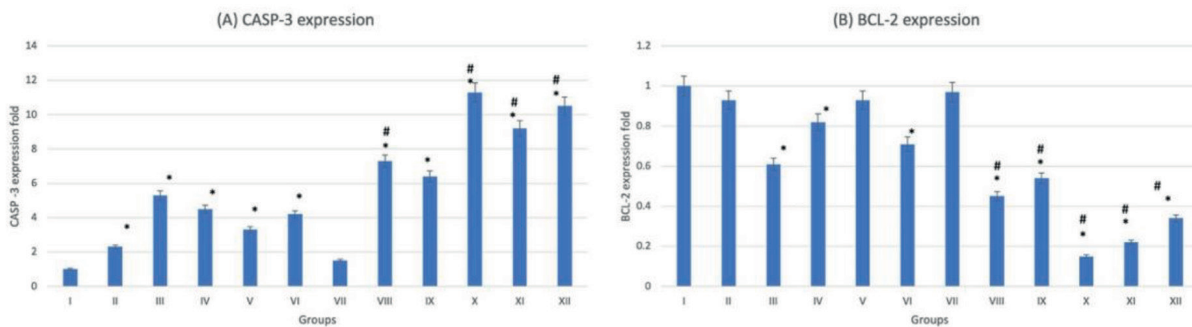


Fig. 13.- Gene expression analysis of the splenic tissue of groups I-XII. (A) represent CASP-3, (B) represent BCL-2. * statistically significant ($p < 0.05$) difference in comparison to I- group. # statistically significant ($p < 0.05$) difference in comparison to VII-group. Data are presented as mean \pm standard deviation, (n=10).

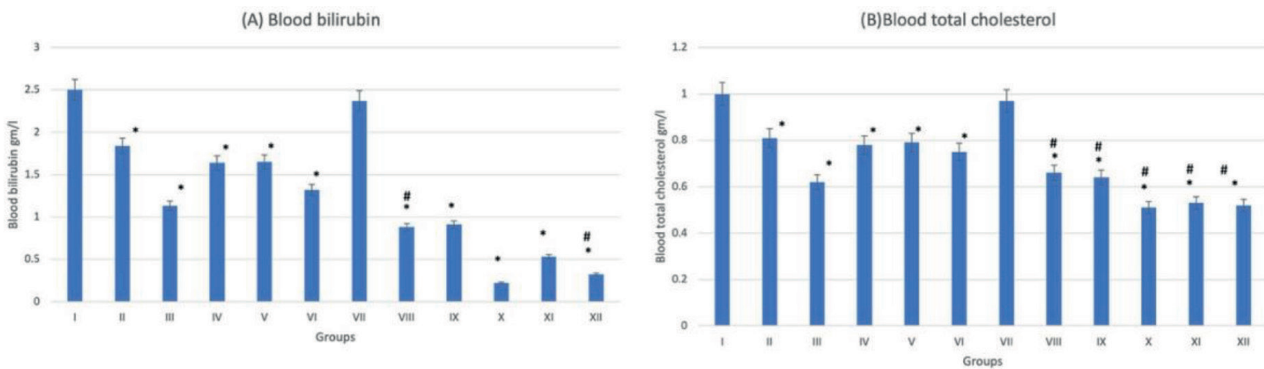


Fig. 14.- Spleen function indicators of groups I-XII. (A) represent blood bilirubin. (B) represent blood total cholesterol. * statistically significant ($p < 0.05$) difference in comparison to I-group. # statistically significant ($p < 0.05$) difference in comparison to VII-group. Data are presented as mean \pm standard deviation, (n=10).

DISCUSSION

Trace metals are naturally found in sea water and earth crust, resulting in frequent exposure rate to these metals and affecting various organs of the body (Di et al., 1968). Diabetes is an endocrinal problem that can also affect many body organs (Sas-Nowosielska and Pawlas, 2015). The present study was conducted to compare between the effect of various trace metals in a diabetic and non-diabetic rat model.

Present results showed that Hg administration to non-diabetic rat groups caused cytoplasmic vacuolation of cardiomyocytes with small pyknotic nuclei and necrosis of cardiac myofibrils, which comes in agreement with Nyland et al. (2012), who reported myocarditis in a clinical case study of Hg toxicity. Other researchers (Ahn et al., 2018) reported that Hg can cause myocarditis. The changes noticed in non-diabetic rats become accentuated in diabetic groups with the appearance of congested blood vessels and capillaries, which was reported by other researchers that mercury causes cardiomyopathy and heart failure (Lombardi et al., 2016).

Gene expression analysis of the heart tissue showed increased expression of CASP-3 (apoptotic gene) while expression of BCL-2 (anti-apoptotic gene) decreased after Hg administration in all rat groups, which collectively favor the apoptotic state of the heart in response to Hg; this comes in agreement with Tiexeira et al. (2016), who reported the apoptotic and toxic effect of mercury on the heart tissue. Ding et al. (2017) mentioned the increased level of mi-RNA 92 in mercury workers, which also favors apoptosis of cells. All these histological findings interfere with the normal function of the heart as stated by Furieri et al. (2011), who reported impaired contractile function of the heart as a result of Hg toxicity. The aortic endothelium as a component of cardiovascular system is also dysfunctional as mentioned by Ahmed and Maulood (2018) in case of Hg toxicity.

The cytoplasmic vacuolations and small pyknotic nuclei appeared also in the kidney tissue beside the congested capillaries of the glomeruli after Hg administration, while other researchers (Li et al., 2011) stated that Hg affect only kidney tubules

with no effect on glomerular capillaries. Seno et al. (2013) added that Hg induced renal injury by inducing autoimmune state. Wang et al. (2015a) agreed with us in the glomerular engagement in the histopathological lesion as he noticed proliferation of mesangial zone of glomeruli. Other researchers (Langworth et al., 1992) agreed with Seno et al. (2013) and mentioned the increased serum antibodies after Hg administration, which result in renal tissue injury.

Our results revealed that the effect of Hg on diabetic rat kidneys is more extensive than the effect on non-diabetic rats, which comes in same page with other researchers (Cohen and Post, 2002), who added that diabetes affect kidney tissue and interferes with urine concentration function, making it more vulnerable to Hg toxic effects. The apoptotic state of the kidney, which was revealed in our research by the fluctuated level of CASP-3 and BCL-2 in favor of CASP-3, was also mentioned by other researchers (Wang et al., 2015b), who explained the apoptotic process which undergoes in the tubular epithelium. Woods et al. (2002) stated that Hg ameliorates NF-KAPPA B, increasing the liability of the renal tissue to apoptosis (Sutton and Tchounwou, 2007). The increased level of urea and creatinine after Hg administration indicate the impairment of kidney functions, which was reported by other researchers (Rojas-Franco et al., 2019) and emphasized our histopathological results of the kidney.

In our study, liver tissue showed cellular degeneration and necrosis together with inflammatory cells infiltration after Hg administration either in diabetic or non-diabetic rats' groups, which appeared as moderate and severe injury respectively. This comes in agreement with other researchers (Chandrasegaran et al., 2018). The increase in expression of CASP-3, which was evident in our results, comes in agreement with Yang et al. (2016), who stated that Hg increases production of reactive oxygen species and causes apoptosis to hepatic cells which is Hg dose dependent.

Lee et al. (2017) reported the relationship between blood mercury concentration and liver function deterioration, which was reported in our results as well. Present results showed that Hg

administration caused shrinkage of B-cells of the pancreas, which appeared with small pyknotic nuclei and cytoplasmic vacuolations: this finding was reported by other researchers (Śliwińska-Mossoń et al., 2018). Present results showed that Hg causes pancreatic inflammation and histological disturbance of both exocrinal and endocrinal components. Chen et al. (2012) reported that Hg increased the production of mi-RNA regulating caspase-3 and caspase-7 production, which comes in agreement with our findings that Hg increases the expression of apoptotic gene CASP-3 and decrease the expression of anti-apoptotic gene BCL-2.

The congested splenic red pulp with wide spread necrosis, which appeared in our results after mercury administrations in diabetic (more extensive pathology) and non-diabetic rats, comes in agreement with other researchers (Ghosh et al., 2018). The increase in expression of apoptotic genes was mentioned by other researchers (Barst et al., 2015), and the disturbed splenic function (immune related) was reported by other researchers (Gill et al., 2017), which comes in agreement with our results after examining splenic functions.

The effect of Ti on cardiac tissue, which appeared in our research, was reported by other researchers (Maublant et al., 1985). The extensive impact of Ti on diabetic rats' heart was explained by Lee and Kim (2017) by occurrence of metabolic disturbance and microvasculature dysfunction. The increase in CASP-3 gene expression recorded in our results was stated by Doue et al. (2008). The histopathological impact of Ti on kidney tissue appeared in our research was stated by (Atkins et al., 1977), who added that Ti is mainly concentrated in the heart, large intestine and kidney. Foster et al. (2012) stated that Ti intake affect mitochondrial functions of the renal tissue, which offer another explanation to the apoptosis rather than the increases expression of CASP-3 gene recorded in our results. In our study, Ti appeared to cause hepatocyte cytoplasmic vacuolation, degeneration and necrosis especially in diabetic group, which was reported by other researchers (Misiakiewicz-Has et al., 2019) who stated that fatty liver insult associated with diabetes mellitus (mainly type -2) makes the liver tissue more liable to the impact of Ti. Apoptosis

of liver cells could be explained due to opposing expression of CASP-3 and BCL-2, while others (Abdel-Daim and Abdou, 2015) stated that Ti cause apoptosis by reactive oxygen species production.

The deterioration of liver functions appeared in our results, especially in diabetic rats, which was reported by Tae et al. (2014) who added that liver cirrhotic states associate Ti toxicity. In present results, Ti caused histopathological changes mainly in diabetic rats, which could be explained by effect of Ti on mitochondria and rough endoplasmic reticulum (Kizilgul et al., 2018). Also, the increase in expression of CASP-3 shown in other results comes in agreement with other researchers (Tekabe et al., 2012). The apoptotic effect of Ti on splenic tissue, which was manifest in our results, was also reported by other researchers (Vasamsetti et al., 2018). Inokuma et al. (1995) reported that high level of Ti tends to accumulate in pancreatic tissue which impacted our results as the pancreas was the most affected organ after Ti administration.

Results showed that Cd administration caused histopathological changes of the heart in the form of cytoplasmic vacuolations and nuclear pyknosis together with necrosis of the cardiac myofibrils, which was expressed more dramatically in the diabetic groups. Sarcomere disorganization and cardiac arrhythmia was reported by Shen et al. (2018) as a result of Cd administration.

Present results showed the relationship between Cd administration and increased CASP-3 expression, which result in cardiomyocytes apoptosis. Nazimabashir et al. (2015) explained Cd-related apoptosis by the activation of Nrf2 apoptotic pathway. The histopathological insult caused by cadmium on both kidney and liver tissue expressed in our results together with increased apoptotic state was also reported by other researchers (Ranieri et al., 2019), who added that the extract of green olive leaf can ameliorate the effect of cadmium on kidney, and they explained apoptosis by the activation of mi-RNA 30 production.

Present results showed histopathological injury of the pancreas and increased expression of CASP-3 gene after Cd administration, especially in diabetic rats, which comes in agreement with other researchers (Śliwińska-Mossoń et al., 2019),

While the disturbed pancreatic function (showed in our result) after Cd administration was not in agreement with Trevino et al. (2015), who linked between the Cd administration and increased insulin secretion. Our results showed that Cd affects mainly the structure, apoptotic activity and function of liver and spleen, which was partially in agreement with Huo et al. (2017), who reported that liver and pancreas are mainly affected after Cd administration.

Cr administration to diabetic and non-diabetic rats, caused histopathological injury to the heart with an increase in CASP-3 gene expression, which comes in agreement with other researchers (Boggelmez and Güvendik, 2019), who elaborated that Cr causes bradycardia in some patients. In our study the kidney reacted to Cr administration by showing disturbed histological architecture, increased apoptosis rate and disturbed renal functions either in diabetic or non-diabetic rats which was reported by other researchers (Venter et al., 2017), who showed that Cr binds to chromatin forcing its condensation mainly on the tubular lining epithelium cells, and reported the occurrence of proteinuria in Cr workers.

Present results showed cytoplasmic vacuolations and necrosis of hepatocytes, increase expression of CASP-3 gene and decrease of liver functions after Cr administration, which comes in agreement with other researchers (Yang et al., 2020), who reported disturbed histological architectures of the liver with disturbed hepatic enzymatic activity after Cr administration. Other researchers (Wang et al., 2017) reported the association between Cr and the histopathological and functional disturbance in the pancreas with increased apoptotic tendency (Same findings were reported in our results). In the present study Cr caused congested red pulp of spleen with cellular necrosis, increased expression of CASP-3 gene and disturbed splenic functions which comes in agreement with (Núñez et al., 2016). Our results showed that the kidney was the most sensitive organ to Cr administration on structural and functional levels, which was confirmed clinically by Filler and McIntyre (2019) in dialysis patients.

Present results showed that, in diabetic and non-diabetic rats, arsenic (As) administration

caused histopathological disturbance and increased expression of CASP-3 gene in the heart tissue. The effect was extensive in diabetic groups if compared to non-diabetic group: this was in the same page with other researchers (Mateen et al., 2017). These histopathological and genetic disturbance was also noticed in the kidney in addition to disturbed function (Sanders et al., 2019). Our study showed that As caused histopathological findings in the liver, pancreas and spleen of non-diabetic rats; more histopathological injury was noticed in diabetic rats (Lu et al., 2019). As administration was associated with increased expression of apoptotic genes and decrease in anti-apoptotic gene expression (Jamal et al., 2020). Present results showed As mainly affected the heart of diabetic rats: this comes in agreement with Wei et al. (2018), who demonstrated the involvement of liver and kidney as well. In conclusion, the present study showed that trace metals are highly toxic to various organs of the body even with low concentration. The diabetic rats are more susceptible to trace-metal-induced cellular damage through gene mediated pathway. The organs insults include structural and functional dimensions. CASP-3 gene plays an important role in trace-metal-associated tissue injury. Cadmium affects mainly hepatic and splenic tissues. Chromium, arsenic and thallium affect mainly the kidney, heart and pancreas respectively.

REFERENCES

- ABDEL-DAIM MM, ABDU RH (2015) Protective effects of diallyl sulfide and curcumin separately against thallium-induced toxicity in rats. *Cell J*, 17(2): 379-388.
- AHMED AH, MAULOOD IM (2018) The roles of potassium channels in contractile response to urotensin-II in mercury chloride induced endothelial dysfunction in rat aorta. *Iran J Vet Res*, 19(3): 208-216.
- AHN H, KIM J, KANG SG, YOON S, KO H-J, KIM P-H, HONG E-J, AN B-S, LEE E, LEE G-S (2018) Mercury and arsenic attenuate canonical and non-canonical NLRP3 inflammasome activation. *Sci Rep*, 8(1): 13659.

ANDREOLI V, SPROVIERI F (2017) Genetic aspects of susceptibility to mercury toxicity: an overview. *Int J Environ Res Public Health*, 14(1): 93.

ASHRAFZADEH S, HAMDY O (2019) Patient-driven diabetes care of the future in the technology era. *Cell Metab*, 29(3): 564-575.

ATKINS HL, BUDINGER TF, LEBOWITZ E, ANSARI AN, GREENE MW, FAIRCHILD RG, ELLIS KJ (1977) Thallium-201 for medical use. Part 3: Human distribution and physical imaging properties. *J Nucl Med*, 18(2): 133-140.

BARST BD, BRIDGES K, KORBAS M, ROBERTS AP, VAN KIRK K, MCNEEL K, DREVNICK PE (2015) The role of melano-macrophage aggregates in the storage of mercury and other metals: an example from yelloweye rockfish (*Sebastes ruberrimus*). *Environ Toxicol Chem*, 34(8):1918-1925.

BETTENCOURT-SILVA R, AGUIAR B, SÁ-ARAÚJO V, BARREIRA R, GUEDES V, MARQUES RIBEIRO MJ, CARVALHO D, ÖSTLUNDH L, SILVA PAULO M (2019) Diabetes-related symptoms, acute complications and management of diabetes mellitus of patients who are receiving palliative care: a protocol for a systematic review. *BMJ Open*, 9(6): e028604.

BEYAERT R, KIDD VJ, CORNELIS S, VAN DE CRAEN M, DENECKER G, LAHTI JM, GURURAJAN R, VANDENABEELE P, FIERS W (1997) Cleavage of PITSLRE kinases by ICE/CASP-1 and CPP32/CASP-3 during apoptosis induced by tumor necrosis factor. *J Biol Chem*, 272(18): 11694-11697.

BOSE-O'REILLY S, BERNAUDAT L, SIEBERT U, ROIDER G, NOWAK D, DRASCH G (2017) Signs and symptoms of mercury-exposed gold miners. *Int J Occup Med Environ Health*, 30(2): 249-269.

BOŞGELMEZ İİ, GÜVENDİK G (2019) Beneficial effects of N-acetyl-L-cysteine or taurine pre- or post- treatments in the heart, spleen, lung, and testis of hexavalent chromium-exposed mice. *Biol Trace Elem Res*, 190(2): 437-445.

CAMPANELLA B, COLOMBAIONI L, BENEDETTI E, DI CIAULA A, GHEZZI L, ONOR M, D'ORAZIO M, GIANNECCHINI R, PETRINI R, BRAMANTI E (2019) Toxicity of thallium at low doses: a review. *Int J Environ Res Public Health*, 16(23): 4732.

CHANDIRASEGARAN G, ELANCHEZHIAN C, GHOSH K (2018) Effects of berberine chloride on the liver of streptozotocin-induced diabetes in albino Wistar rats. *Biomed Pharmacother*, 99: 227-236.

CHEN KL, LIU SH, SU CC, YEN CC, YANG CY, LEE KI, TANG FC, CHEN YW, LU TH, SU YC, HUANG CF (2012) Mercuric compounds induce pancreatic islets dysfunction and apoptosis in vivo. *Int J Mol Sci*, 13(10): 12349-12366.

COHEN M, POST GS (2002) Water transport in the kidney and nephrogenic diabetes insipidus. *J Vet Intern Med*, 16(5): 510-517.

DI LOLLO F, FAZZINI G, MORINI PL (1968) Diabete e complicanze encefaliche acute a genesi dismetabolica. Attuali aspetti patogenetici e fisiopatologici [Diabetes and acute dysmetabolic encephalic complications. Current pathogenetic and physiopathological aspects]. *Recenti Prog Med*, 44(2): 178-212.

DING E, GUO J, BAI Y, ZHANG H, LIU X, CAI W, ZHONG L, ZHU B (2017) MiR-92a and miR-486 are potential diagnostic biomarkers for mercury poisoning and jointly sustain NF- κ B activity in mercury toxicity. *Sci Rep*, 7(1): 15980.

DOUE T, OHTSUKI K, OGAWA K, UEDA M, AZUMA A, SAJI H, STRAUSS HW, MATSUBARA H (2008) Cardioprotective effects of erythropoietin in rats subjected to ischemia-reperfusion injury: assessment of infarct size with 99mTc-annexin V. *J Nucl Med*, 49(10): 1694-1700.

EL-BADRY A, REZK M, EL-SAYED H (2018) Mercury-induced oxidative stress may adversely affect pregnancy outcome among dental staff: a cohort study. *Int J Occup Environ Med*, 9(3): 113-119.

FILLER G, MCINTYRE C (2019) Chromium: rise and shine in peritoneal dialysis patients? *Perit Dial Int*, 39(4): 320-322.

FOSTER DB, HO AS, RUCKER J, GARLID AO, CHEN L, SIDOR A, GARLID KD, O'ROURKE B (2012) Mitochondrial ROMK channel is a molecular component of mitoK(ATP). *Circ Res*, 111(4): 446-454.

FURIERI LB, FIORESI M, JUNIOR RF, BARTOLOMÉ MV, ARAÚJO FERNANDES A, CACHO-

- FEIRO V, LAHERA V, SALAICES M, STEFANON I, VASSALLO DV (2011) Exposure to low mercury concentration in vivo impairs myocardial contractile function. *Toxicol Appl Pharmacol*, 255(2): 193-199.
- GHOSH S, CHOWDHURY S, SARKAR P, SIL PC (2018) Ameliorative role of ferulic acid against diabetes associated oxidative stress induced spleen damage. *Food Chem Toxicol*, 118: 272-286.
- GILARDI F, WINKLER C, QUIGNODON L, DISERENS JG, TOFFOLI B, SCHIFFRIN M, SARDELLA C, PREITNER F, DESVERGNE B (2019) Systemic PPAR γ deletion in mice provokes lipotrophy, organomegaly, severe type 2 diabetes and metabolic inflexibility. *Metabolism*, 95: 8-20.
- GILL R, MCCABE MJ JR, ROSENSPIRE AJ (2017) Low level exposure to inorganic mercury interferes with B cell receptor signaling in transitional type 1 B cells. *Toxicol Appl Pharmacol*. 330: 22-29.
- HUO J, DONG A, YAN J, WANG L, MA C, LEE S (2017) Cadmium toxicokinetics in the freshwater turtle, *Chinemys reevesii*. *Chemosphere*, 182: 392-398.
- HWANG JS, DAHMS HU, HUANG KL, HUANG MY, LIU XJ, KHIM JS, WONG CK (2018) Bioaccumulation of trace metals in octocorals depends on age and tissue compartmentalization. *PLoS One*, 13(4): e0196222.
- INOKUMA T, TAMAKI N, TORIZUKA T, FUJITA T, MAGATA Y, YONEKURA Y, OHSHIO G, IMAMURA M, KONISHI J (1995) Value of fluorine-18-fluorodeoxyglucose and thallium-201 in the detection of pancreatic cancer. *J Nucl Med*, 36(2): 229-235.
- JAMAL Z, DAS J, GHOSH S, GUPTA A, CHATTOPADHYAY S, CHATTERJI U (2020) Arsenic-induced immunomodulatory effects disorient the survival-death interface by stabilizing the Hsp90/Beclin1 interaction. *Chemosphere*, 238: 124647.
- KARBOWSKA B (2016) Presence of thallium in the environment: sources of contaminations, distribution and monitoring methods. *Environ Monit Assess*, 188(11): 640.
- KERN JK, GEIER DA, SYKES LK, HALEY BE, GEIER MR (2016) The relationship between mercury and autism: A comprehensive review and discussion. *J Trace Elem Med Biol*, 37: 8-24.
- KIZILGUL M, WILHELM JJ, BEILMAN GJ, CHINNAKOTLA S, DUNN TB, PRUETT TL, ABDULLA M, HELLER D, FREEMAN ML, SCHWARZENBERG SJ, HERING BJ, BELLIN MD (2018) Effect of intrapancreatic fat on diabetes outcomes after total pancreatectomy with islet autotransplantation. *J Diabetes*, 10(4): 286-295.
- LANGWORTH S, ELINDER CG, SUNDQUIST KG, VESTERBERG O (1992) Renal and immunological effects of occupational exposure to inorganic mercury. *Br J Ind Med*, 49(6): 394-401.
- LEE MR, LIM YH, LEE BE, HONG YC (2017) Blood mercury concentrations are associated with decline in liver function in an elderly population: a panel study. *Environ Health*, 16(1): 17.
- LEE WS, KIM J (2017) Diabetic cardiomyopathy: where we are and where we are going. *Korean J Intern Med*, 32(3): 404-421.
- LI SJ, ZHANG SH, CHEN HP, ZENG CH, ZHENG CX, LI LS, LIU ZH (2010) Mercury-induced membranous nephropathy: clinical and pathological features. *Clin J Am Soc Nephrol*, 5(3): 439-444.
- LOMBARDI C, SPIGONI V, GORGA E, DEI CAS A (2016) Novel insight into the dangerous connection between diabetes and heart failure. *Herz*, 41(3): 201-207.
- LU P, MA JQ, LI F, XU GH, GUO W, ZHOU HM (2019) A fatal case of acute arsenic poisoning. *J Forensic Sci*, 64(4): 1271-1273.
- MATEEN FJ, GRAU-PEREZ M, POLLAK JS, MOON KA, HOWARD BV, UMANS JG, BEST LG, FRANCESCINI KA, GOESSLER W, CRAINICEANU C, GUALLAR E, DEVEREUX RB, ROMAN MJ, NAVASACIEN A (2017) Chronic arsenic exposure and risk of carotid artery disease: The strong heart study. *Environ Res*, 157: 127-134.
- MAUBLANT JC, MOINS N, GACHON P, ROSS MR, DAVIDSON WD, MENAI (1985) Effects of grisorixin on the distribution of thallium-201 and on the oxidative metabolism in cultured myocardial cells. *J Nucl Med*, 26(6): 626-629.
- MISIAKIEWICZ-HAS K, MACIEJEWSKA D, KOLASA-WOŁOSIUK A, PILUTIN A, RZESZOTEK S, WILK A, SZYPULSKA-KOZIARSKA D, STACHOWSKA E, ŁUKOMSKA A, WISZNIEWSKA B (2019)

Modulatory effect of inulin with soya isoflavones on plasma lipid profile and liver SCD-18 index in rats with induced type-2 diabetes mellitus. *Histol Histopathol*, 34(10): 1131-1140.

NAZIMABASHIR, MANOHARAN V, MILTONPRABU S (2015) Cadmium induced cardiac oxidative stress in rats and its attenuation by GSP through the activation of Nrf2 signaling pathway. *Chem Biol Interact*, 242: 179-193.

NÚÑEZ O, FERNÁNDEZ-NAVARRO P, MARTÍN-MÉNDEZ I, BEL-LAN A, LOCUTURA JF, LÓPEZ-ABENTE G (2016) Arsenic and chromium topsoil levels and cancer mortality in Spain. *Environ Sci Pollut Res Int*, 23(17): 17664-17675.

NYLAND JF, FAIRWEATHER D, SHIRLEY DL, DAVIS SE, ROSE NR, SILBERGELD EK (2012) Low-dose inorganic mercury increases severity and frequency of chronic coxsackievirus-induced autoimmune myocarditis in mice. *Toxicol Sci*, 125(1): 134-143.

PAWŁOWSKA M, LEGUTKO D, STEFANIUK M (2017) Zajrzyć w głąb mózgu - nowe techniki oczyszczania optycznego i obrazowania z zastosowaniem mikroskopu arkusza światła [Getting an insight into the brain - new optical clearing techniques and imaging using light-sheet microscope]. *Postepy Biochem*, 63(1): 8-15.

PIEPOLI MF, HOES AW, AGEWALL S, ALBUS C, BROTONS C, CATAPANO AL, COONEY MT, CORRÀ U, COSYNS B, DEATON C, GRAHAM I, HALL MS, HOBBS FDR, LØCHEN ML, LÖLLGEN H, MARQUES-VIDAL P, PERK J, PRESCOTT E, REDON J, RICHTER DJ, SATTAR N, SMULDERS Y, TIBERI M, VAN DER WORP HB, VAN DIS I, VERSCHUREN WMM, BINNO S (2016) European Guidelines on cardiovascular disease prevention in clinical practice: The Sixth Joint Task Force of the European Society of Cardiology and Other Societies on Cardiovascular Disease Prevention in Clinical Practice (constituted by representatives of 10 societies and by invited experts). Developed with the special contribution of the European Association for Cardiovascular Prevention & Rehabilitation (EACPR). *Eur Heart J*, 37(29): 2315-2381.

RANIERI M, DI MISE A, DIFONZO G, CENTRONE M, VENNERI M, PELLEGRINO T, RUSSO A, MAS-

TRODONATO M, CAPONIO F, VALENTI G, TAMMA G (2019) Green olive leaf extract (OLE) provides cytoprotection in renal cells exposed to low doses of cadmium. *PLoS One*, 14(3): e0214159.

ROJAS-FRANCO P, FRANCO-COLÍN M, TORRES-MANZO AP, BLAS-VALDIVIA V, THOMPSON-BONILLA MR, KANDIR S, CANO-EUROPA E (2019) Endoplasmic reticulum stress participates in the pathophysiology of mercury-caused acute kidney injury. *Ren Fail*, 41(1): 1001-1010.

SANDERS AP, MAZZELLA MJ, MALIN AJ, HAIR G, BUSGANG SA, SALAND JM, CURTIN P (2019) Combined exposure to lead, cadmium, mercury, and arsenic and kidney health in adolescents age 12-19 in NHANES 2009-2014. *Environ Int*, 131: 104993.

SAS-NOWOSIELSKA H, PAWLAS N (2015) Heavy metals in the cell nucleus - role in pathogenesis. *Acta Biochim Pol*, 62(1): 7-13.

SENO K, OHNO J, OTA N, HIROFUJI T, TANIGUCHI K (2013) Lupus-like oral mucosal lesions in mercury-induced autoimmune response in Brown Norway rats. *BMC Immunol*, 14: 47.

SHEN J, WANG X, ZHOU D, LI T, TANG L, GONG T, SU J, LIANG P (2018) Modelling cadmium-induced cardiotoxicity using human pluripotent stem cell-derived cardiomyocytes. *J Cell Mol Med*, 22(9): 4221-4235.

SIBLERUD R, MUTTER J, MOORE E, NAUMANN J, WALACH H (2019) A hypothesis and evidence that mercury may be an etiological factor in Alzheimer's disease. *Int J Environ Res Public Health*, 16(24): 5152.

ŚLIWIŃSKA-MOSSOŃ M, MILNEROWICZ S, MILNEROWICZ H (2018) Diabetes mellitus secondary to pancreatic diseases (type 3c): The effect of smoking on the exocrine-endocrine interactions of the pancreas. *Diab Vasc Dis Res*, 15(3): 243-259.

ŚLIWIŃSKA-MOSSOŃ M, SOBIECH K, DOLEZYCH B, MADEJ P, MILNEROWICZ H (2019) N-acetyl-beta-D-glucosaminidase in tissues of rats chronically exposed to cadmium and treated with ozone. *Ann Clin Lab Sci*, 49(2): 193-203.

SUTTON DJ, TCHOUNWOU PB (2007) Mercury induces the externalization of phosphatidyl-ser-

ine in human renal proximal tubule (HK-2) cells. *Int J Environ Res Public Health*, 4(2): 138-144.

TAE HJ, JUN DW, CHOI YY, KWAK MJ, LEE MH (2014) Assessment of risk of complications in cirrhosis using portal thallium scans. *World J Gastroenterol*, 20(1): 228-234.

TEIXEIRA FB, DE OLIVEIRA ACA, LEÃO LKR, FAGUNDES NCF, FERNANDES RM, FERNANDES LMP, DA SILVA MCF, AMADO LL, SAGICA FES, DE OLIVEIRA EHC, CRESPO-LOPEZ ME, MAIA CSF, LIMA RR (2018) Exposure to inorganic mercury causes oxidative stress, cell death, and functional deficits in the motor cortex. *Front Mol Neurosci*, 11: 125.

TEKABE Y, LUMA J, LI Q, SCHMIDT AM, RAMASAMY R, JOHNSON LL (2012) Imaging of receptors for advanced glycation end products in experimental myocardial ischemia and reperfusion injury. *JACC Cardiovasc Imaging*, 5(1): 59-67.

THEM TR II, GILL BC, CARUTHERS AH, GERHARDT AM, GRÖCKE DR, LYONS TW, MARROQUÍN SM, NIELSEN SG, TRABUCHO ALEXANDRE JP, OWENS JD (2018) Thallium isotopes reveal protracted anoxia during the Toarcian (Early Jurassic) associated with volcanism, carbon burial, and mass extinction. *Proc Natl Acad Sci USA*, 115(26): 6596-6601.

TREVIÑO S, WAALKES MP, FLORES HERNÁNDEZ JA, LEÓN-CHAVEZ BA, AGUILAR-ALONSO P, BRAMBILA E (2015) Chronic cadmium exposure in rats produces pancreatic impairment and insulin resistance in multiple peripheral tissues. *Arch Biochem Biophys*, 583: 27-35.

VASAMSETTI SB, FLORENTIN J, COPPIN E, STIEKEMA L, ZHENG KH, NISAR MU, SEMBRAT J, LEVINTHAL D, ROJAS M, STROES ES, KIM K, DUTTA P (2018) Sympathetic neuronal activation triggers myeloid progenitor proliferation and differentiation. *Immunity*, 49(1): 93-106.e7.

VENTER C, OBERHOLZER HM, CUMMINGS FR, BESTER MJ (2017) Effects of metals cadmium and chromium alone and in combination on the liver and kidney tissue of male Sprague-Dawley rats: An ultrastructural and electron-energy-loss spectroscopy investigation. *Microsc Res Tech*, 80(8): 878-888.

VIANNA ADS, MATOS EP, JESUS IM, ASMUS CIRF, CÂMARA VM (2019) Human exposure to mercury

and its hematological effects: a systematic review. *Cad Saude Publica*, 35(2): e00091618.

WANG C, CHEN Z, PAN Y, GAO X, CHEN H (2017) Anti-diabetic effects of Inonotus obliquus polysaccharides-chromium (III) complex in type 2 diabetic mice and its sub-acute toxicity evaluation in normal mice. *Food Chem Toxicol*, 108(Pt B): 498-509.

WANG Y, WANG D, WU J, WANG B, GAO X, WANG L, MA H (2015a) Cinnabar-induced subchronic renal injury is associated with increased apoptosis in rats. *Biomed Res Int*, 2015: 278931.

WANG Y, WANG D, WU J, WANG B, WANG L, GAO X, HUANG H, MA H (2015b) Cinnabar induces renal inflammation and fibrogenesis in rats. *Biomed Res Int*, 2015: 280958.

WEI H, HU Q, WU J, YAO C, XU L, XING F, ZHAO X, YU S, WANG X, CHEN G (2018) Molecular mechanism of the increased tissue uptake of trivalent inorganic arsenic in mice with type 1 diabetes mellitus. *Biochem Biophys Res Commun*, 504(2): 393-399.

WESTERBERG DP (2013) Diabetic ketoacidosis: evaluation and treatment. *Am Fam Physician*, 87(5): 337-346.

WOODS JS, DIEGUEZ-ACUÑA FJ, ELLIS ME, KUSHLEIKA J, SIMMONDS PL (2002) Attenuation of nuclear factor kappa B (NF-kappaB) promotes apoptosis of kidney epithelial cells: a potential mechanism of mercury-induced nephrotoxicity. *Environ Health Perspect*, 110 (Suppl 5): 819-822.

WU M, SHU Y, SONG L, LIU B, ZHANG L, WANG L, LIU Y, BI J, XIONG C, CAO Z, XU S, XIA W, LI Y, WANG Y (2019) Prenatal exposure to thallium is associated with decreased mitochondrial DNA copy number in newborns: Evidence from a birth cohort study. *Environ Int*, 129: 470-477.

YANG D, TAN X, LV Z, LIU B, BAIYUN R, LU J, ZHANG Z (2016) Regulation of Sirt1/Nrf2/TNF- α signaling pathway by luteolin is critical to attenuate acute mercuric chloride exposure induced hepatotoxicity. *Sci Rep*, 6: 37157.

YANG Y, WANG W, LIU X, SONG X, CHAI L (2020) Probing the effects of hexavalent chromium exposure on histology and fatty acid metabolism in liver of *Bufo gargarizans* tadpoles. *Chemosphere*, 243: 125437.